Enhanced topological superconductivity in an asymmetrical planar Josephson junction

Erhu Zhang(张二虎) and Yu Zhang(张钰)†

Department of Applied Physics, School of Science, Xi'an Jiaotong University, Xi'an 710049, *China*

(Received 8 August 2022; revised manuscript received 4 December 2022; accepted manuscript online 9 December 2022)

As a platform for holding Majorana zero models (MZMs), the two-dimensional planar topological Josephson junction that can be used as carriers for topological quantum computing faces some challenges. One is a combination of mirror and time-reversal symmetries may make the system hold multiple pairs of MZMs. The other is that a soft gap dominated by a large momentum occurs in a clean system. To solve these problems, asymmetric junction can be introduced. Breaking this symmetry changes the symmetry class from class BDI to class D, and only a single pair of MZMs can be left at the boundary of the system. We numerically study four cases that create an asymmetric system and find out different superconducting pairing potential, different coupling coefficients between two-dimensional electron gases (2DEGs) and two superconducting bulks, different widths of two superconducting bulks make the gap of the system decrease at the optimal value, but make the gap at the minimum value increases. And the zigzag-shape quasi-one-dimensional junction eliminates the large momentum parallel to the junction and enhances the gap at the large momentum. However, the zigzag-shape junction cannot increase the gap at the region of multiple pairs of MZMs in a symmetric system. We show that by combining zigzag-shape junction with different coupling coefficients, the system can maintain a large gap ($\approx 0.2\Delta$) in a wide region of the parameter space.

Keywords: topological superconductivity, planar Josephson junction, Majorana zero modes

PACS: 03.67.Lx, 74.78.–w, 74.45.+c **DOI:** 10.1088/1674-1056/acaa29

1. Introduction

As the most promising candidate for topological quantum computing, Majorana zero model (MZM) has received the widespread attention in recent years.[1–10] Earlier schemes proposed to create MZMs focus on the one-dimensional systems with strong spin–orbit interaction and proximity-induced superconductivity,[11–21] including proximitized semiconductor nanowires[22–29] and ferromagnetic atomic chains.[30,31] The existence of MZM is proved by the appearance of zero bias conductance peak in most experiments.[11–36] Recently, an alternative promising platform for the creation and manipulation of MZMs has been proposed, which is a two-dimensional planar Josephson junction based on a 2DEG with strong Rashba spin–orbit coupling in proximity to two superconducting bulks, as shown in Fig. 1(a). In this system, superconducting phase difference φ provides an additional control knob that can enhance the parameter space leading to topological superconductivity. And the MZMs appear at the end of the quasi-one-dimensional junction which is between two superconducting bulks, as shown in Fig. 1(b). At present, several groups have fabricated the junctions experimentally and demonstrated that they support topological superconductivity over a large range of parameters.[37–44]

However, creating stable MZM in a planar Josephson junction system also faces challenges, one is the appearance of multiple pairs of MZMs at the boundary of the system. Symmetry classes of tenfold way are characterized by the presence or absence of time-reversal, particle–hole and chiral symmetries. If the Hamiltonian only respects particle–hole symmetry and the particle–hole operator $U_{\rm P} = \sigma_y\tau_y K$ square to 1, the system is in symmetry class D. When the Hamiltonian respects time-reversal, particle–hole and chiral symmetries, the time-reversal operator square to 1 and the particle–hole operator square to 1, the system is in symmetry class BDI. The Hamiltonian of our model respects time-reversal symmetry without Zeeman field and with a phase difference of 0 or π. Meanwhile, if the system does not have disorder along the x direction, which is perpendicular to the junction, the Hamiltonian of the system commutes with a mirror operator M_x with respect to the y–z plane. When applying a magnetic field along the junction and the phase difference between the two superconducting bulks is not 0 or π, both of these symmetries are broken, but the Hamiltonian of system commutes with their product, i.e., there is an antiunitary effective time-reversal symmetry operator $U_T = M_x T$, where $T = {\rm i}\sigma_y K$ (with K denoting complex conjugation). In addition, the particle–hole symmetry presents, and chiral symmetry also presents. The chiral symmetry is $C = -{\rm i}U_T U_{\rm P}$. The existence of the three symmetries — effective time-reversal symmetry, particle–hole symmetry and chiral symmetry — ensure that the system is no longer D symmetry class but belongs to the higher-symmetry BDI class. The BDI symmetry class is characterized by an integer invariant $W_{\mathbb{Z}}$, which represents the number of MZMs on a single end. Therefore, multiple pairs of MZMs can appear in the system. And another challenge is soft gap caused by large momentum. For this system, the gap of low momen-

†Corresponding author. E-mail: 646907259@qq.com

© 2023 Chinese Physical Society and IOP Publishing Ltd

tum is $\min(\Delta, h v_F/W)$, where v_F is the electron Fermi velocity and W is the width of the junction. While large-momentum k_y closes to k_F in a system without disorder, there has a long trajectories length and a long flight time τ_F, the gap is approximately $\hbar^2/\left(2m_e W^2\right)$, where m_e is the effective mass.[45,48] At present, the topological gap observed in most experiments is soft gap rather than hard gap.[41–44]

In order to obtain robust topological phase that can be used in topological quantum computation experimentally, many researchers put forward several theoretical suggestions. On the one hand, some asymmetric cases are proposed, such as applying a transverse in-plane magnetic field, weak disorder that breaks the mirror symmetry, different superconducting pairing potentials and different widths of superconducting bulks.[45,49] It is beneficial for topological quantum computing to break the U_T symmetry. When BDI symmetry class is broken, the system reduces to the D symmetry class.[45,49] And the D class is characterized by a topological invariant $W_{\mathbb{Z}_2}$. The multiple pairs of MZMs at the boundary of the system hybridize in pairs and turn into the finite-energy modes. Only a single pair of MZMs can be left on the boundary of the system. On the other hand, weak disorder and a zigzag-shape junction are proposed for the elimination of large momentum in Refs. [46,48]. However, there are still some problems with the proposals. According to the Ref. [47], applying a transverse field reduces the gap significantly. Although weak disorder can decrease the MZM localization length and make the topological phase robust, it is impossible to control to the required precision experimentally.[48] Therefore, it is necessary to systematically discuss the topological gap of these asymmetric systems.

In this paper, we summarize the three cases mentioned above that create an asymmetric system, which are different superconducting pairing potentials, different widths of two superconducting bulks and zigzag-shape quasi-one-dimensional junction. In addition, we propose to make the different coupling coefficients between 2DEGs and two superconducting bulks. We numerically simulate the energy spectra of these four cases based on the tight binding model, and observe that multiple pairs of MZMs hybridize because the BDI symmetry class is broken. Through numerical simulation of topological gap at infinite size, we can observe the close of the gap at phase transition point in BDI topological class and the reopening of the gap in D topological class. By comparison, it can be found that with the increase of the degree of asymmetry, the topological gap of the system significantly increases at the gap closing points (which signify the BDI phase transition), but decreases slightly at the φ close to the optimal value, when the system has different superconducting pairing potentials or different widths of superconducting bulks or different coupling coefficients. This means that the dependence of topological gap on φ decreases under fixed magnetic field. Relatively speaking, the difference of coupling coefficients has the most obvious improvement when the degree of asymmetry is low. In contrast, zigzag-shape junction increases the gap at the optimal value, but remains a small value at the regions of multiple pairs of MZMs. Finally, we discuss the case of combination of zigzag-shape junction with different coupling coefficients, and find through numerical simulation that the system can maintain a large gap in a wide parameter space in this case.

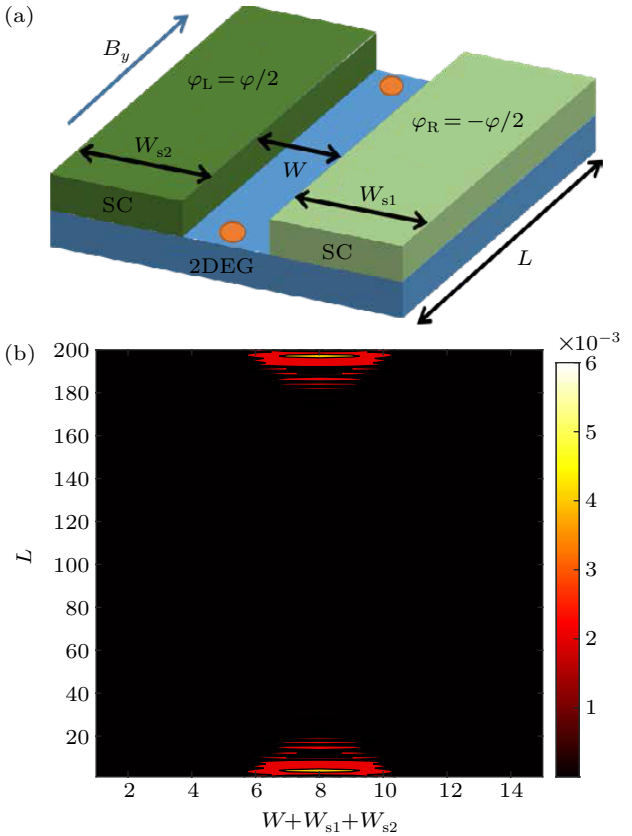


Fig. 1. (a) Illustration of a planar Josephson junction with different parameters of the superconducting bulks on different sides. The blue part represents 2DEG with strong Rashba spin–orbit coupling. The dark and the light green part represent superconducting bulks covered on the 2DEG. Dark green and light green mean that two superconducting bulks have different parameters, such as width and coupling coefficient, etc. When adjusting parameters to make the system enter non-trivial topological states, MZMs appear at the end of the junction, represented by two orange dots. And panel (b) shows the local density of states of the MZMs. The figure was obtained by using a tight-binding model with the following parameters: $W = 5$, $W_{s1} = W_{s2} = 5$, $L = 200$, $t = 1$, $\alpha = 0.5$, $\mu = -2.75$, $\Delta_1 = \Delta_2 = 0.3$, $E_Z = 0.6$.

2. Model and formula

Figure 1(a) shows the model of a topological planar Josephson junction. The bottom layer is the 2DEG with strong Rashba spin–orbit coupling, the 2DEG is covered with a thin layer of superconductor on the left and right side. The tight-binding model of this system can be read as

$$H_{TB} = H_0 + H_{soc} + H_Z + H_\Delta, \tag{1}$$

$$H_0 = -\mu \sum_{sij} \psi^\dagger_{i,j,s} \psi_{i,j,s} - t \sum_{(ij,i'j')s} \left[\psi^\dagger_{i,j,s} \psi_{i',j',s} + \text{H.C.} \right], \tag{2}$$

$$H_{\mathrm{SOC}}=\mathrm{i}\alpha\sum_{s,s'}\left[\sum_{i=1}^{W_{\mathrm{S1}}+W+W_{\mathrm{S2}}-1}\sum_{j=1}^{L}\psi_{i+1,j,s}^{\dagger}\sigma_{y}^{s,s'}\psi_{i,j,s'}-\sum_{i=1}^{W_{\mathrm{S1}}+W+W_{\mathrm{S2}}}\sum_{j=1}^{L-1}\psi_{i,j+1,s}^{\dagger}\sigma_{x}^{s,s'}\psi_{i,j,s'}-\mathrm{H.C.}\right], \quad (3)$$

$$H_{\mathrm{Z}}=E_{\mathrm{Z}}\sum_{iss'}\sum_{i=W_{\mathrm{S1}}+1}^{W_{\mathrm{S1}}+W}\psi_{i,j,s}^{\dagger}\sigma_{x}^{s,s'}\psi_{i,j,s'}+\mathrm{H.C.}, \quad (4)$$

$$H_{\Delta}=\Delta\,\mathrm{e}^{-\mathrm{i}\varphi/2}\sum_{i=1}^{W_{\mathrm{S1}}}\sum_{j}\psi_{i,j,\uparrow}\psi_{i,j,\downarrow}+\Delta\,\mathrm{e}^{\mathrm{i}\varphi/2}\sum_{i=W_{\mathrm{S1}}+W+1}^{W_{\mathrm{S1}}+W+W_{\mathrm{S2}}}\sum_{j}\psi_{i,j,\uparrow}\psi_{i,j,\downarrow}+\mathrm{H.C.}, \quad (5)$$

where $\psi_{(i,j,s)}$ is the annihilation operator of an electron with spin s on site (i,j), and $(ij,i'j')$ denotes nearest neighbor. In Eq. (2), t is the hopping amplitude, μ is the chemical potential of 2DEG and the superconducting bulks. In the next two equations, α represents the Rashba spin–orbit coupling strength of 2DEG, E_{Z} represents the strength of Zeeman energy. Here we argue that superconducting bulks have no Zeeman field according to the Meissner effect. E_{Z} exists only in the junction. And the last equation represents the superconducting pairing in the 2DEG, which comes from the proximity effect of the left (right) superconducting bulk. And the superconducting pairing amplitude Δ is only nonzero when $x>W/2$ or $x<-W/2$. Furthermore, i and j denote the lattice site, while $\uparrow$ and $\downarrow$ are the spin indices.

When the model has additional symmetry, it belongs to the BDI symmetry class. At some E_{Z}, the system undergoes multiple topological phase transitions with varying phase difference. In order to observe the information of topological phase transition more intuitively, we calculate topological invariants $W_{\mathbb{Z}}$ (BDI) according to the Ref. [50]. The topological properties are obtained from a corresponding bulk system. To perform a partial Fourier transform to extend the junction to infinite length in the y direction. Because the Hamiltonian anticommutes with chiral operator, the Hamiltonian can be written in off-diagonal formal

$$C=\begin{pmatrix}1&0\\0&-1\end{pmatrix},\quad H=\begin{pmatrix}0&A\\A^{\dagger}&0\end{pmatrix}. \quad (6)$$

The topological invariant $W_{\mathbb{Z}}$ of the class BDI can be calculated from the phase of the determinant of A. The Hamiltonian is characterized by a function $z(k)=\exp(\mathrm{i}\theta(k))=\mathrm{Det}(A(k))/|\mathrm{Det}(A(k))|$. The invariant $W_{\mathbb{Z}}=(-\mathrm{i})/\pi\int_{k=0}^{k=\pi}\mathrm{d}z(k)/z(k)$.

We compute $W_{\mathbb{Z}_2}$ in the standard way by representing $H(k_y)$ as a matrix $M(k_y)$ in Majorana representation[1]

$$H(k_y)=\frac{\mathrm{i}}{2}\sum_{\eta\eta' ss' xx'}M_{x\eta s,x'\eta' s'}|x\eta s\rangle\langle x'\eta' s'|. \quad (7)$$

The topological invariant can be given by

$$W_{\mathbb{Z}_2}=\mathrm{sgn}\frac{\mathrm{Pf}(M(k_y=0))}{\mathrm{Pf}(M(k_y\to\infty))}, \quad (8)$$

where Pf denotes the Pfaffian.

3. Results and discussion

In this section, we first discuss the case of different superconducting pairing potentials at fixed E_{Z} proposed in Ref. [45], Δ_1 is not equal to Δ_2. To observe the appearance and disappearance of multiple pairs of MZMs, we select parameters $W=5$, $W_{\mathrm{s1}}=W_{\mathrm{s2}}=5$, $L=200$, $t=1$, $\alpha=0.5$, $\mu=-2.75$, which are used in Ref. [45]. In Fig. 2, the energy spectra with 50 eigenvalues versus varying phase difference φ were calculated when $\Delta_1=\Delta_2=0.3$, $\Delta_1=0.2$, $\Delta_2=0.4$, and $\Delta_1=0.1$, $\Delta_2=0.5$, respectively. It can be seen that the system is non-trivial in all values of the phase difference when Zeeman field is 0.6. As shown in Fig. 2(a), when the superconducting pairing potentials are the same, the system belongs to BDI symmetry class and undergoes more than one phase transition with increasing phase difference. At $\varphi<0.14\pi$, $W_{\mathbb{Z}}=3$ corresponds to the emergence of three pairs of MZMs in the topological gap, and the gap decreases and closes at 0.14π. When the φ is larger than 0.14π, the gap is reopened, leaving a single pair of zero energy state, $W_{\mathbb{Z}}=1$. The dotted lines in Fig. 2(a) represent the phase transition points of the system. The gap has been closed and reopened several times and the values of $W_{\mathbb{Z}}$ in different regions are marked in Fig. 2(a), while the values of $W_{\mathbb{Z}}$ are all odd. In order to avoid the influence of finite size effect on gap, gap is calculated under infinite length and the closing and opening of gap can be easily observed. The gap of the system is determined by the lowest energy Andreev bound state E_{A}. Figures 2(d)–2(f) show the corresponding bulk E_{gap} ($E_{\mathrm{gap}}=\min(E_{\mathrm{A}}(k_y))$) at different φ. When different superconducting pairing potentials are given in the model, the BDI symmetry class reduces to D class, and the zero energy states are coupled to each other and leave a single pair of zero energy states. Thus, the system is non-trivial at all values of phase difference in Figs. 2(b) and 2(c), and the gap is always open. According to Fig. 2(d), it can be seen that when $E_{\mathrm{Z}}=0.6$ in the model, the optimal value of gap appears at $\varphi=\pi$, while the minimum values of gap are at the gap closing points. When the system belongs to the D symmetry class, the phase difference φ of the optimal value of gap does not change, while the φ of minimum values of gap shift from gap closing points to $\varphi=2N\pi$ (N is an integer) with the increase of the degree of asymmetry, see Figs. 2(e) and 2(f). The different superconducting pairing potentials make the minimum values of gap increase, but reduce the optimal value of gap at some extent. And the higher the degree of asymmetry is, the smaller the optimal value of the gap is. In the limiting case, $\Delta_2=0$. This system can be seen as the absence of the right side. When the value of Δ_2 is infinitely close to zero, the optimal value of the gap is much smaller than that of the optimal value of the symmetry system. These are consistent with the results of Refs. [45,47].

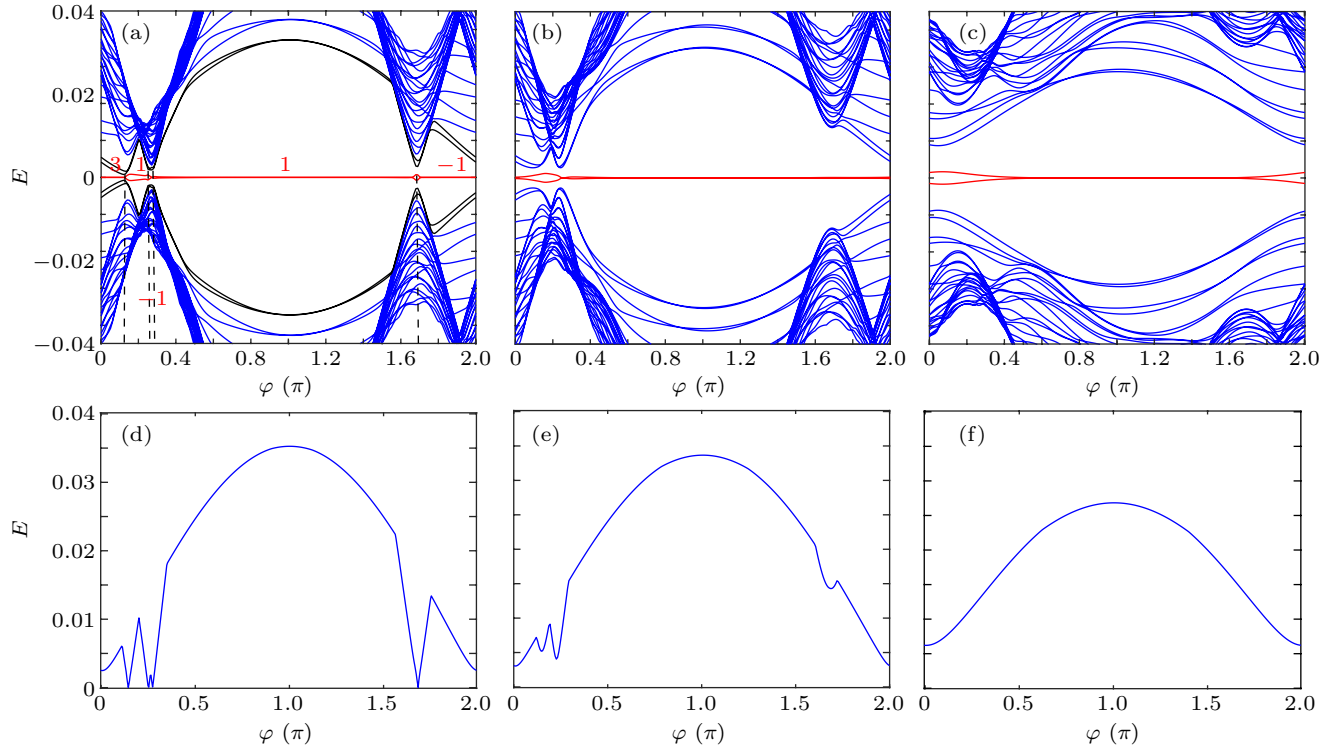


Fig. 2. Energy spectra as a function of phase difference φ with different superconducting pairing potentials. (a) $\Delta_1 = \Delta_2 = 0.3$. (b) $\Delta_1 = 0.2$, $\Delta_2 = 0.4$. (c) $\Delta_1 = 0.1$, $\Delta_2 = 0.5$. The red lines represent the zero energy states. In panel (a), the black lines represent the appearance and disappearance of the MZMs with varying φ and the dotted lines show the phase transition points of the class BDI system. Panels (d)–(f) are the corresponding bulk $E_{\rm gap}$ ($E_{\rm gap} = \min(E(k_y))$ at different φ. The gap of the system is determined by the lowest energy in all k_y. When $\Delta_1 = \Delta_2 = 0.3$, the system has several gap closing points, while $\Delta_1 = 0.2$, $\Delta_2 = 0.4$, and $\Delta_1 = 0.1$, $\Delta_2 = 0.5$ the gap is open at all values of φ. Other parameters are $W = 5$, $W_{\rm s1} = W_{\rm s2} = 5$, $L = 200$, $t = 1$, $\alpha = 0.5$, $\mu = -2.75$, and $E_{\rm Z} = 0.6$.

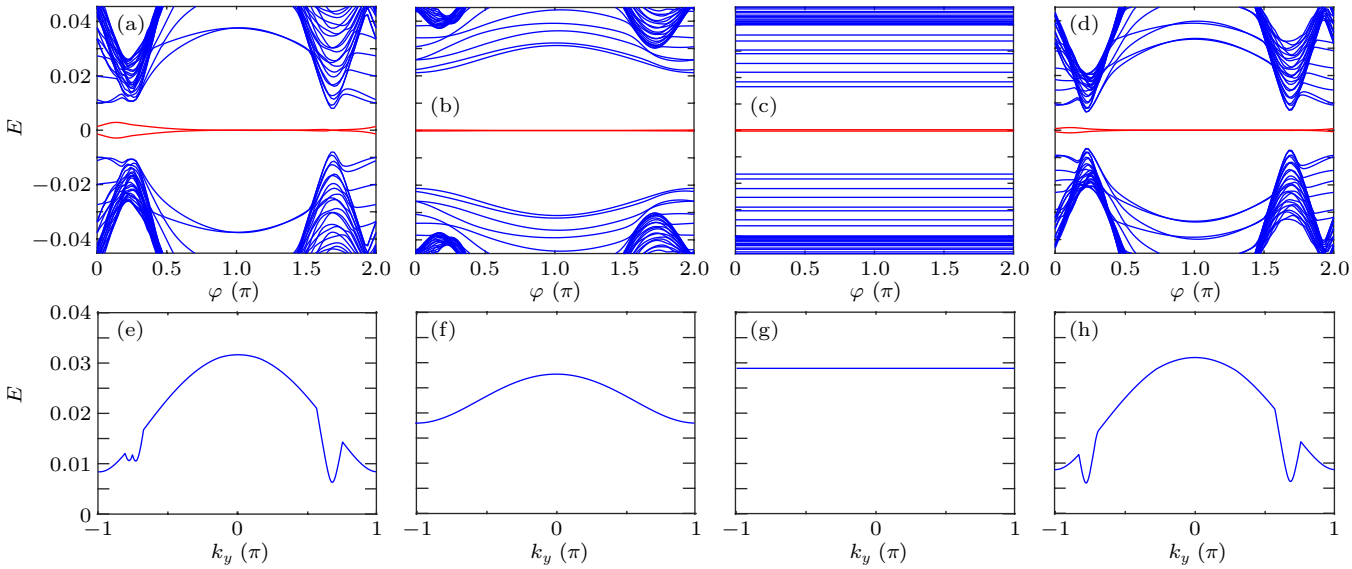


Fig. 3. Energy spectra as a function of phase difference φ with different coupling coefficients between superconducting bulks and junction. The parameters describing the coupling strength are (a) $t_{\rm c1} = t_{\rm c2} = 1$, (b) $t_{\rm c1} = 1$, $t_{\rm c2} = 0.9$, (c) $t_{\rm c1} = 1$, $t_{\rm c2} = 0.7$, (d) $t_{\rm c1} = 1$, $t_{\rm c2} = 0$. When the coupling coefficient $t_{\rm c2}$ decreases, the superconducting tunneling rate decreases, which makes the gap induced by the proximity effect smaller, it may be assumed that the coupling coefficient decreases in the same proportion as the superconducting pairing potential, $t_{\rm c2} = 0.9$, $\Delta_1 = 0.3$, $\Delta_2 = 0.27$. Panels (e)–(h) are the corresponding bulk $E_{\rm gap}$ with varying φ. Other parameters are $W = 5$, $W_{\rm s1} = W_{\rm s2} = 5$, $L = 200$, $\alpha = 0.5$, $\mu = -2.75$, $\Delta_1 = \Delta_2 = 0.3$, and $E_{\rm Z} = 0.6$.

Next, we consider a case that two superconducting bulks on either side of the junction have different coupling coefficients with the junction. Here, the parameters describing the coupling strength of the left and the right superconductors need to be defined, which are represented by $t_{\rm c1}$ and $t_{\rm c2}$ (by default $t_{\rm c1} = t_{\rm c2} = 1$ if there is no special indication elsewhere), i.e., modifying Eq. (2) with the following:

$$t\sum_{j=1}^{L}\left[t_{\rm c1}\psi^{\dagger}_{W_{\rm s1},j,s}\psi_{W_{\rm s1}+1,j,s} + t_{\rm c2}\psi^{\dagger}_{W_{\rm s1}+W,j,s}\psi_{W_{\rm s1}+W+1,j,s} + \text{H.C.}\right]. \tag{9}$$

Other parameters should be fixed in accordance with the pre-

vious ones. Figure 3 shows that the energy spectra with the varying phase difference at fixed $t_{c1} = 1$ and variable t_{c2}. It can be seen that the symmetry class reduces to D class so long as t_{c1} is not equal to t_{c2}. The gap is always opened at all values of phase difference and there only has a single pair of zero energy states. Compared with the case of different superconducting pairing potentials, as t_{c2} decreases, the gap at the optimal value has a smaller decreasing value. The reduction of the coupling coefficient means that the transmission probability is lower, resulting in a lower Andreev reflection amplitude. When $t_{c2} < 0.5$, the energy spectra with varying φ becomes flat. Figure 3(c) shows spectrum without oscillation. The situation that $t_{c2} = 0$ means that there is no superconducting bulk on the right side of the system. It is easy to understand that the phase of a single superconductor has no physical effect.

As a further consideration, the effect of the reduction of the coupling coefficient in the system may not be so onefold. When the coupling coefficient t_{c2} decreases, the superconducting tunneling rate decreases, which makes the gap induced by the proximity effect smaller, that is to say, the decrease of t_{c2} is accompanied by the decrease of Δ_2. Figure 3(d) shows the spectrum with varying phase difference at $t_{c2} = 0.9$ and $\Delta_2 = 0.27$. It can be seen that in all values of φ, the system can hold a stable single pair of MZMs, and there has a largest gap at $\varphi = \pi$. As discussed above, this case has little effect on the gap in the optimal value, it is beneficial to keep the stability of the single pair of MZMs and a certain size of the gap by making the coupling coefficients between the superconducting bulks and junction different.

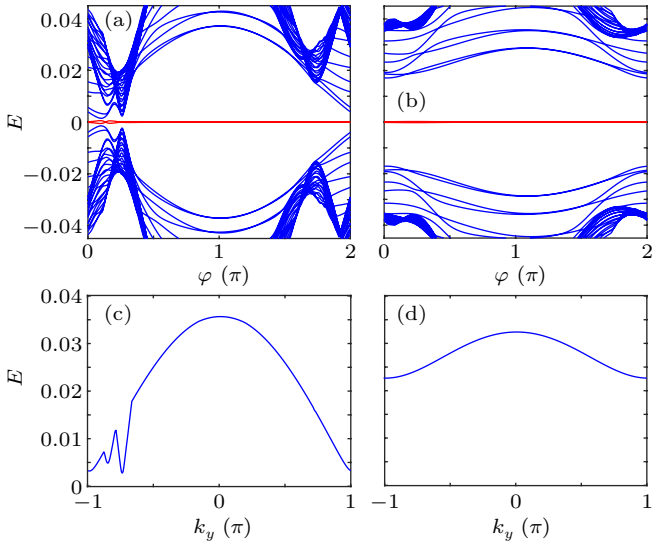


Fig. 4. Energy spectra as a function of phase difference φ with different coupling coefficients between superconducting bulks and junction. The parameters are $W_{s1} = 5$, (a) $W_{s2} = 4$, (b) $W_{s2} = 1$, $\Delta_1 = \Delta_2 = 0.3$. Panels (c)–(d) are the corresponding bulk E_{gap} with varying φ. Other parameters are $W = 5$, $L = 200$, $t = 1$, $\alpha = 0.5$, $\mu = -2.75$, $\Delta_1 = \Delta_2 = 0.3$, and $E_Z = 0.6$.

The third case we discussed is to make the widths of two superconducting bulks different, i.e., W_{s1} is not equal to W_{s2}. As shown in Fig. 4, the different values of W_s also eliminate the presences of multiple pairs of MZMs, which has the same mechanism as the two cases mentioned above, and the gap at the minimum value increases with the decrease of the width of superconducting bulk. Compared with the different coupling coefficients, the effect of different widths of superconducting bulks on gap is weaker, and there has strong dependency between φ and bulk energy before the width of superconducting bulk decreases to zero. When we take the value of W_{s1}/W_{s2} to the limit value 0, it is consistent with $t_{c2} = 0$.

Through the above discussion, we find that changing the parameters of the left and the right superconducting bulks can only make the minimum value of gap larger and close to the optimal value of gap by the same mechanism, in other words, they both make the energy spectrum diagram and topological gap independent of the phase difference in the limiting case.[47] But this class of asymmetry does not eliminate soft gap due to large momentum. Reference [46] proposed a zigzag-shape junction with the same mechanism as weak disorder, which is to cut off the long trajectories with a large momentum. Figure 5(a) shows the schematic diagram of zigzag-shape junction. The peak-to-peak amplitude is denoted by Z_x. The period length of a zigzag-shape is denoted by Z_y. Figures 5(c) and 5(d) show that the spectra of parallel junction and zigzag-shape junction with varying phase difference at $L = 300$, respectively. In order to observe the information of gap more intuitively, Figs. 5(b), 5(e), and 5(f) are band structures of the system at $\varphi = \pi$. When the straight trajectories are completely cut off, the energy spectrum becomes insensitive to momentum and the band flattens out ($Z_x = W$), see Figs. 5(c) and 5(d). The energy at large-momentum $k_y \approx k_F$ increases and the increased gap reduces the localization length of the MZM. Thus, the energy splitting caused by the limited wave function overlap is reduced. In addition, it can be seen from Figs. 5(c) and 5(d) that the zigzag-shape junction increases gap significantly only around the optimal value of gap. For the regions where multiple pairs of MZMs occur in a symmetric system, gap cannot increase. This case reduces the topological regions of robust MZMs at fixed E_Z.

Another noteworthy point is that too short Z_y makes the angle between the junction and the magnetic field larger, decreasing the gap of low momentum, as shown in Fig. 6(a). However, too long Z_y cannot cut off the long trajectories with a large momentum, as shown in Fig. 6(c). The optimal value of Z_y should be between $3W$ and $10W$, as shown in Fig. 6(b).

Although the zigzag-shape junction eliminates the soft gap caused by large momentum, the gap with low momentum is still limited by the width of junction. Figure 7 shows the band structures of the narrow junction. It can be seen that when the width of junction is smaller than that of the coherence length, the gap can reach 0.06 even in the case of the straight junction.[51,52] When the width of junction is small, the gap of the zigzag-shape junction can also remain near 0.06. Therefore, a zigzag-shape junction can be constructed to maintain the optimal value of gap for both wide and narrow junction.

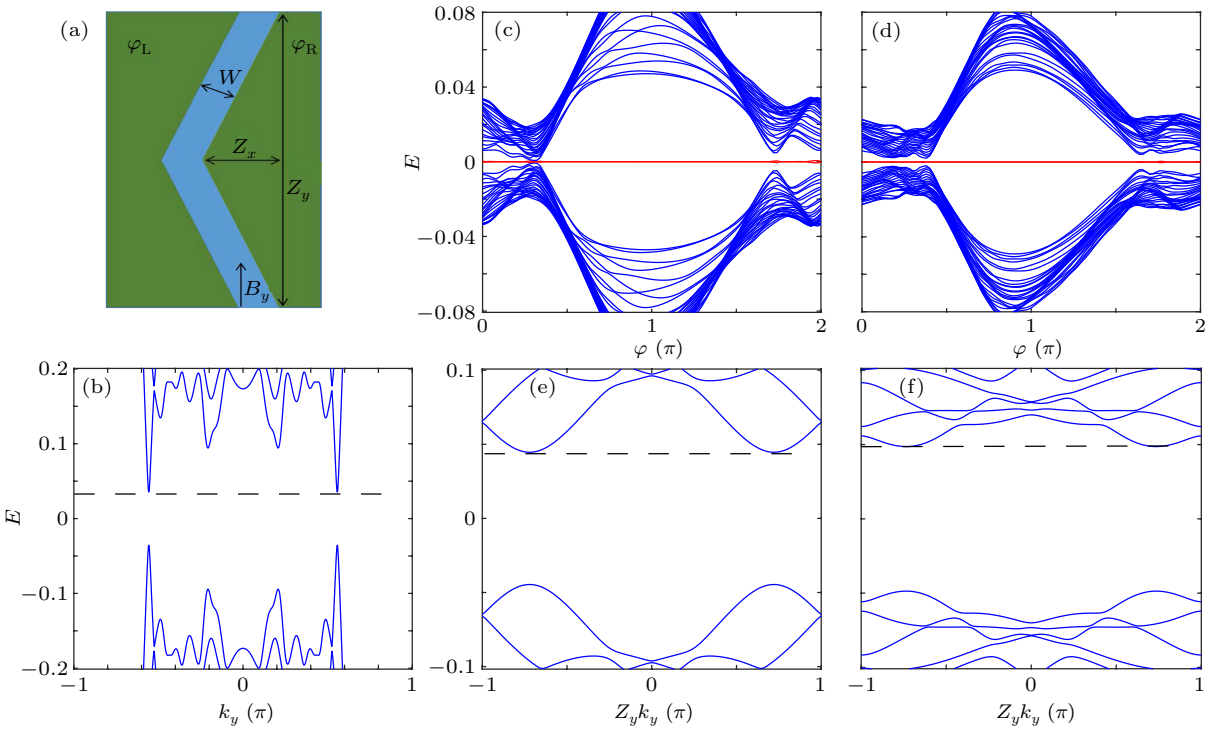


Fig. 5. (a) Illustration of a planar Josephson junction with a shape of zigzag. (b) The straight band structure at different momenta k_y at $\varphi = \pi$. Energy spectra are functions of phase difference φ with different Z_x in (c) $Z_x = W/2$, (d) $Z_x = W$. Panels (e)–(f) are the corresponding band structure at different momenta k_y at $\varphi = \pi$, $Z_y = 6W$. Other parameters are $W = 5$, $W_{s1} = W_{s2} = 5$, $L = 200$, $t = 1$, $\alpha = 0.5$, $\mu = -2.75$, $\Delta_1 = \Delta_2 = 0.3$, and $E_Z = 0.6$.

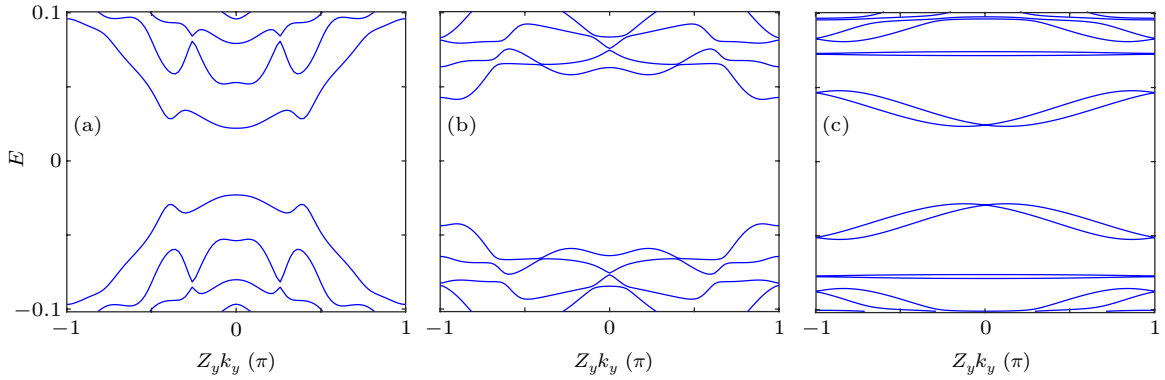


Fig. 6. Band structures of the system at $Z_x = W$ and $\varphi = \pi$. (a) $Z_y = 2W$, (b) $Z_y = 4W$, (c) $Z_y = 16W$. Other parameters are $W = 5$, $W_{s1} = W_{s2} = 5$, $L = 200$, $t = 1$, $\alpha = 0.5$, $\mu = -2.75$, $\Delta_1 = \Delta_2 = 0.3$, and $E_Z = 0.6$.

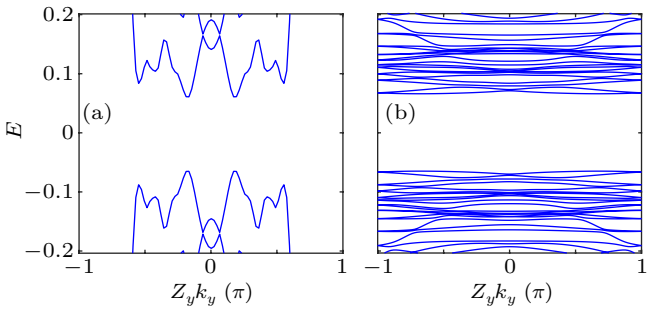


Fig. 7. (a) Band structures of the straight junction at $W = 2$. (b) Band structures of the corresponding zigzag-shape junction at $Z_x = W$ and $Z_y = 6W$. Other parameters are $W = 5$, $W_{s1} = W_{s2} = 5$, $L = 200$, $t = 1$, $\alpha = 0.5$, $\mu = -2.75$, $\Delta_1 = \Delta_2 = 0.3$, and $E_Z = 0.6$.

Finally, we numerically simulate E_{gap} as a function of Zeeman field and phase difference, as can be seen in Fig. 8. Figure 8(a) shows E_{gap} versus Zeeman field and phase difference in the symmetry case. The results of superconducting pairing potential, coupling coefficient and the width of superconducting bulks are similar. Taking only the superconducting pairing potential as an example, Fig. 8(b) shows the E_{gap} versus Zeeman field and phase difference when $\Delta_1 = 0.5$ and $\Delta_2 = 0.1$, respectively. In Fig. 8(b), the gap in the topological region is weakly dependent on Zeeman field and phase difference, and it is a stable and broad topological region. For the zigzag-shape junction, the topological gap only increases in a small region of the parameter space and the gap cannot be improved in the regions where multiple pairs of MZMs occur in a symmetric system, as can be seen in Fig. 8(c).[46] Consider further the case where asymmetry is combined with a zigzag junction. According to the above discussion, the coupling co-

efficient can significantly increase the gap when the degree of asymmetry is low. Figure 8(d) is obtained by combining the zigzag-shape junction with different coupling coefficients. It can be seen that in this case, the system can obtain the gap that the value can reach 0.2Δ and large robust topological phase region.

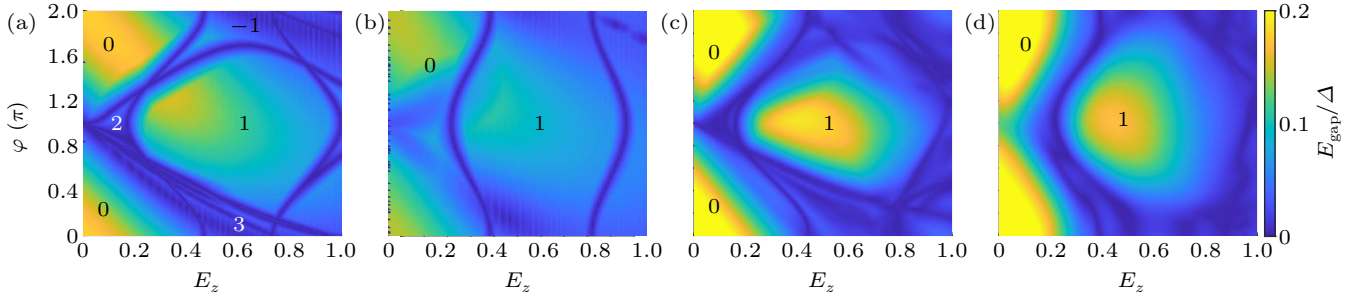


Fig. 8. The gap is shown as a function of the Zeeman energy E_Z and phase difference φ (a) in the symmetry case, (b) in the different superconducting pairing potentials, i.e., $\Delta_1 = 0.5$, $\Delta_2 = 0.1$, (c) in the zigzag-shape junction, $Z_x = W$, $Z_y = 6W$, (d) in the combination of zigzag-shape junction and different coupling coefficients, i.e., $t_{c1} = 1$, $t_{c2} = 0.5$. Other parameters are $W = 5$, $W_{s1} = W_{s2} = 5$, $L = 200$, $t = 1$, $\alpha = 0.5$, $\mu = -2.75$, $\Delta_1 = \Delta_2 = 0.3$. We insert partial number of MZMs in the figures.

4. Conclusion

We summarize four cases to enhance the topological gap of MZMs in planar Josephson junctions. For the ideal topological superconductor for quantum computing, we hope to have a single pair of MZMs at the ends of the junction and a large topological gap. Different superconducting pairing potentials, coupling coefficients and widths of junction can break the additional symmetry and increase the minimum value of gap. They reduce the dependence of the single pair of MZMs and topological gap on phase difference. According to the above discussion, it is easy to see that a significant improvement of gap can occur with a low degree of asymmetry by adjusting the coupling coefficient. Zigzag-shape junction can improve the size of the gap by eliminating large momentum. Both the wide junction and narrow junction can maintain a lager value of gap. However, the options of zigzag-shape junction require a certain level of material preparation, and the choice of ideal gap depends on the period of Z_y and the size of Z_x. In addition, the zigzag-shape junction does not improve the gap in the regions where multiple pairs of MZMs occur in a symmetric system, which makes the robust topological phase region smaller. Therefore, we propose to combine the zigzag-shape junction with different coupling coefficients to obtain large gap and robust topological phase region. Our numerical simulation provides a new possibility for the experimental preparation of stable single pair of MZMs.

Acknowledgment

Project supported by the National Natural Science Foundation of China (Grant No. 11974271).

References

[1] Kitaev A Y 2001 *Phys. Usp.* **44** 131
[2] Kitaev A Y 2003 *Ann. Phys.* **303** 2
[3] Nayak C, Simon S H, Stern A, Freedman M and Das Sarma S 2008 *Rev. Mod. Phys.* **80** 1083
[4] Alicea J 2012 *Rep. Prog. Phys.* **75** 076501
[5] Elliott S R and Franz M 2015 *Rev. Mod. Phys.* **87** 137
[6] Leijnse M and Flensberg K 2012 *Semicond. Sci. Technol.* **27** 124003
[7] Das Sarma S, Freedman M and Nayak C 2015 *NPJ Quantum Inform.* **1** 15001
[8] Beenakker C and Kouwenhoven L 2016 *Nat. Phys.* **12** 618
[9] Aguado R 2017 *Riv. Nuovo Cim.* **40** 523
[10] Chen W Q, Wang J C, Wu Y J, Qi J J, Liu J and Xie X C 2022 *Phys. Rev. B* **105** 054507
[11] Fu L and Kane C L 2008 *Phys. Rev. Lett.* **100** 096407
[12] Sau J D, Lutchyn R M, Tewari S and Das Sarma S 2010 *Phys. Rev. Lett.* **104** 040502
[13] Fujimoto S 2008 *Phys. Rev. B* **77** 220501
[14] Sato M, Takahashi Y and Fujimoto S 2010 *Phys. Rev. B* **82** 134521
[15] Alicea J 2010 *Phys. Rev. B* **81** 125318
[16] Lutchyn R M, Sau J D and Das Sarma S 2010 *Phys. Lett.* **105** 077001
[17] Oreg Y, Refael G and Von Oppen F 2011 *Phys. Rev. Lett.* **105** 177002
[18] Potter A C and Lee P A 2011 *Phys. Rev. B* **83** 094525
[19] Klinovaja J, Stano P, Yazdani A and Loss D 2013 *Phys. Rev. Lett.* **111** 186805
[20] Nadj-Perge S, Drozdov I K, Bernevig B A and Yazdani A 2013 *Phys. Rev. B* **88** 020407
[21] Lutchyn R M, Bakkers E P A M, Kouwenhoven L P, Krogstrup P, Marcus C M and Oreg Y 2018 *Nat. Rev. Mater.* **3** 52
[22] Chang W, Albrecht S M, Jespersen T S, Kuemmeth F, Krogstrup P, Nygård J and Marcus C M 2015 *Nat. Nanotechnol.* **10** 232
[23] Mourik V, Zuo K, Frolov S M, Plissard S R, Bakkers E P A M and Kouwenhoven L P 2012 *Science* **336** 1003
[24] Deng M T, Yu C L, Huang G Y, Larsson M, Caroff P and Xu H Q 2012 *Nano Lett.* **12** 6414
[25] Das A, Ronen Y, Oreg Y, Heiblum M and Shtrikman H 2012 *Nat. Phys.* **8** 887
[26] Fabrizio N, Asbjørn C C D, Alexander M W, Eoin C T O'Farrell, Henri J Suominen, Antonio F, Tian W, Gardner G C, Candice T, Anthony T Hatke, Krogstrup P, Manfra M J, Flensberg K and Marcus C M 2017 *Phys. Rev. Lett.* **119** 136803
[27] Önder G, Zhang H, Bommer J D S, de Moor M W A, Car D, Plissard S R, Bakkers E P A M, Geresdi A, Watanabe K, Taniguchi T and Kouwenhoven L P 2018 *Nat. Nanotechnol.* **13** 192
[28] Zhang H, Liu C X, Gazibegovic S, Xu D, Logan J A, Wang G Z, Nick van Loo, Bommer J D S, de Moor M W A, Car D, Op het Veld R L M, Petrus J van Veldhoven, Koelling S, Verheijen M A, Pendharkar M, Pennachio D J, Shojaei B, Lee J S, Palmstrom C J, Bakkers E P A M, Das Sarma S and Kouwenhoven L P 2018 *Nature* **556** 74
[29] Albrecht S M, Higginbotham A P, Madsen M, Kuemmeth F, Jespersen T S, Nygard J, Krogstrup P and Marcus C M 2016 *Nature* **531** 206

[30] Nadj-perge S, Drozdov I K, Li J, Chen H, Jeon S, Seo J, Allan H. MacDonald, Bernevig B A and Yazdani A 2014 *Science* **346** 602

[31] Feldman B E, Randeria M T, Li J, Jeon S, Xie Y L, Wang Z J, Drozdov I K, Andrei Bernevig B and Yazdani A 2014 *Nat. Phys.* **13** 286

[32] Bommer J D S, Zhang H, Gül Ö, Nijholt B, Wimmer M, Rybakov F N, Garaud J, Rodic D, Babaev E, Troyer M, Car D, Plissard S R, Bakkers E P A M, Watanabe K, Taniguchi T and Kouwenhoven L P 2019 *Phys. Rev. Lett.* **122** 187702

[33] Sun H H, Zhang K W, Hu L H, Li C, Wang G Y, Ma H Y, Xu Z A, Gao C L, Guan D D, Li Y Y, Liu C, Qian D, Zhou Y, Fu L, Li S C, Zhang F C and Jia J F 2016 *Phys. Rev. Lett.* **116** 257003

[34] Wang D F , Kong L Y, Fan P, Chen H, Zhu S Y, Liu W Y, Cao L, Sun Y J, Du S X, Schneeloch J, Zhong R D, Gu G D, Fu L, Ding H and Gao H J 2018 *Science* **362** 333

[35] Qin L, Chen C, Tong Z, *et al.* 2018 *Phys. Rev. X* **8** 041056

[36] Peng Z, Koichiro Y, Takahiro H, Yuichi O, Takeshi K, Kozo O, Wang Z J, W J S, Gu G D, Hong D and Shin S 2018 *Science* **360** 182

[37] Farrell E C T O, Drachmann A C C, HelI M, Fornieri A, Whiticar A W, Hansen E B, Gronin S, Gardner G C, Thomas C, Manfra M J, Flensberg K, Marcus C M and Nichele F 2018 *Phys. Rev. Lett.* **121** 256803

[38] Joon S L, Borzoyeh S, Mihir P, Anthony P M, Younghyun K, Henri J S, Morten K, Fabrizio N, Hao Z, Charles M M and Chris J P 2019 *Nano Lett.* **19** 3083

[39] William M, William F S, Joseph Y, Mehdi H, Wendy L S, Stefan P S, Asher C, Leff T C, Kaushini S Wickramasinghe, Matthieu C Dartiailh, Igor Ž and Javad S 2020 *ACS Appl. Electron. Mater.* **2** 2351

[40] Pankratova N, Lee H, Kuzmin R, Wickramasinghe K, Maye W Y J, Vavilov M G, Shabani J and Manucharyan V E 2020 *Phys. Rev. X* **10** 031051

[41] Dartiailh M C, Mayer W, Yuan J, Wickramasinghe K S, Matos-Abiague A, Zutic I and Shabani J 2012 *Phys. Rev. Lett.* **126** 036802

[42] Moehle C M, Ke C T, Wang Q Z, Thomas C, Di Xiao, Karwal S, Lodari M, Vincent van de Kerkhof, Termaat R, Gardner G C, Scappucci G, Manfra M J and Goswami S 2021 *Nano Lett.* **21** 9990

[43] Fornieri A, Whiticar A M, Setiawan F, Portolés E, Drachmann A C C, Keselman A, Gronin S, Thomas C, Wang T, Kallaher R, Gardner G C, Berg E, Manfra M J, Stern A, Marcus C M and Nichele F 2019 *Nature* **569** 89

[44] Ren H, Pientka F, Hart S, Pierce A, Kosowsky M, Lunczer L, Schlereth R, Scharf B, Hankiewicz E M, Molenkamp L W, Halperin B I and Yacoby A 2019 *Nature* **569** 93

[45] Pientka F, Keselman A, Berg E, Yacob A, Stern A and Halperin B I 2017 *Phys. Rev. X* **7** 021023

[46] Tom L, Bas N, Michael W and Anton R A 2020 *Phys. Rev. Lett.* **125** 086802

[47] Setiawan F, Ady S and Erez B 2019 *Phys. Rev. B* **99** 220506

[48] Haim A and Stern A 2019 *Phys. Rev. Lett.* **122** 126801

[49] Hell M, Leijnse M and Flensberg K 2017 *Phys. Rev. Lett.* **118** 107701

[50] Tewari S and Sau J D 2012 *Phys. Rev. Lett.* **109** 150408

[51] Setiawan F, Wu C T and Levin K 2019 *Phys. Rev. B* **99** 174511

[52] Zhang Y, Guo K and Liu J 2020 *Phys. Rev. B* **102** 245403